

## Fundamental free-space solutions of a steady axisymmetric MHD viscous flow

A. Sellier<sup>a</sup> and S. H. Aydin<sup>b</sup>

<sup>a</sup>LadHyX, Ecole Polytechnique, Palaiseau, France; <sup>b</sup>Department of Mathematics, Karadeniz Technical University, Trabzon, Turkey.

### ABSTRACT

This work obtains the velocity and pressure fields of two fundamental *axisymmetric* MHD viscous flows of a conducting Newtonian liquid due to axial and radial distributions of forces on a ring in the presence of a uniform axial magnetic field  $\mathbf{B} = B\mathbf{e}_z$ . The worked out procedure rests on the analytical determination of the pressure and of some of the Cartesian velocity components of another general three-dimensional fundamental MHD flow. The derived axisymmetric fundamental flows are found to deeply depend upon the nature (axial or radial) of the forces distributed on the ring, the ring size and the Hartmann layer thickness  $d = (\sqrt{\mu/\sigma})/|B|$ . This is illustrated by computing a few flow patterns using a suitable numerical treatment.

### ARTICLE HISTORY

Received 20 October 2015  
Accepted 28 February 2016

### KEYWORDS

MagnetoHydrodynamics;  
Lorentz body force;  
axisymmetric flow;  
Green's flow; circular  
shape source

## 1. Introduction

For some basic applications, it is required to determine the flow about a solid (either insulating or conducting) body experiencing a given rigid-body migration in a conducting Newtonian liquid subject to a uniform and steady ambient magnetic field  $\mathbf{B}_0$ . In general, the body affects the ambient magnetic field and in addition to the disturbed magnetic field  $\mathbf{B}$  a non-uniform electric field  $\mathbf{E}$ , vanishing far from the body, also arises in the liquid. The occurring liquid flow, with velocity  $\mathbf{u}$  and pressure  $p$ , is driven by the Lorentz body force  $\mathbf{f} = \mathbf{j} \wedge \mathbf{B}$  with a current density  $\mathbf{j}$  adopting for usual cases the Ohm's law  $\mathbf{j} = \sigma(\mathbf{E} + \mathbf{u} \wedge \mathbf{B})$  where  $\sigma > 0$  designates the uniform liquid conductivity. For a solid rigid migration described by its translational velocity  $\mathbf{U}$  and angular velocity  $\boldsymbol{\Omega}$  one then looks at the quantities  $(\mathbf{B}, \mathbf{E}, \mathbf{u}, p)$  in the entire liquid domain once the body shape and motion  $(\mathbf{U}, \boldsymbol{\Omega})$ , the uniform ambient magnetic field  $\mathbf{B}_0$  and the liquid uniform conductivity  $\sigma > 0$ , density  $\rho$  and viscosity  $\mu$  are provided. Such a task turns out to be tremendously involved because the fields  $(\mathbf{B}, \mathbf{E}, \mathbf{u}, p)$  are governed by the unsteady *non-linear and coupled* Maxwell and Navier–Stokes equations with non-uniform Lorentz body force  $\mathbf{f} = \sigma(\mathbf{E} + \mathbf{u} \wedge \mathbf{B}) \wedge \mathbf{B}$ . For further informations regarding this challenging issue falling inside the so-called and wide field of

Magnetohydrodynamics, the reader is directed to (Branover & Tsinober, 1970; Tsinober, 1970; Moreau, 1990).

If one restricts the attention to a small enough particle experiencing a slow motion, the problem becomes quasi-steady but still difficult to solve even for the case of a sphere (Gotoh, 1960). As nicely discussed and summarised in Gotoh (1960), for a steady problem several great simplifications, detailed below, might however occur depending upon the range of some dimensionless numbers and/or upon the problem symmetries. Those relevant dimensionless numbers are defined using the body length scale  $a$ , the flow velocity magnitude scale  $V > 0$  and the liquid uniform conductivity  $\sigma > 0$ , density  $\rho$ , viscosity  $\mu$  and magnetic permeability  $\mu_m > 0$ . The very first number is the magnetic Reynolds number  $\text{Re}_m = \mu_m \sigma Va$ . As in most of the encountered cases, we henceforth assume that  $\text{Re}_m \ll 1$  and the body to have the same magnetic permeability as the liquid. It follows (Tsinober, 1970) that  $\mathbf{B} = \mathbf{B}_0$  in the entire liquid domain, with magnitude  $B = |\mathbf{B}| > 0$ . Near the body surface a so-called Hartmann layer (Hartmann, 1937), with typical thickness  $d = (\sqrt{\mu/\sigma})/B$ , takes place. In this layer, the viscous term  $\mu \nabla^2 \mathbf{u}$  and the flow contribution  $\sigma (\mathbf{u} \wedge \mathbf{B}) \wedge \mathbf{B}$  to the Lorentz body force have comparable magnitudes. Two additional key dimensionless numbers are then introduced: the Reynolds number  $\text{Re}$  and the so-called Hartmann number  $M$  defined as

$$\text{Re} = \rho Va/\mu, \quad M = a/d = aB/\sqrt{\mu/\sigma}. \quad (1)$$

Note that  $M$  compares the body length scale  $a$  with the Hartmann layer thickness  $d$  and that  $M$  vanishes with the ambient magnetic field  $\mathbf{B}$ . Getting this time the steady fields  $(\mathbf{E}, \mathbf{u}, p)$  whatever  $(\mathbf{B}, \text{Re}, M)$  and the body shape and rigid-body migration  $(\mathbf{U}, \mathbf{\Omega})$  is therefore still a challenging task essentially because the electric field  $\mathbf{E}$  is coupled with the velocity field  $\mathbf{u}$  in the entire liquid domain through the equations  $\nabla \wedge \mathbf{E} = \mathbf{0}$  and  $\nabla \cdot \mathbf{E} = -(\nabla \wedge \mathbf{u}) \cdot \mathbf{B}$  (with the latter relation provided by the charge conservation in steady case  $\nabla \cdot \mathbf{j} = 0$ ). Fortunately, this coupling vanishes due to symmetries in the following basic and quite different cases:

- (i) The two-dimensional MHD flow about a plane solid body with  $\mathbf{B}$  and  $\mathbf{u}$  lying in the same plane.
- (ii) The axisymmetric three-dimensional MHD flow about a solid body of revolution translating, without rotating, with  $\mathbf{U}$  and  $\mathbf{B}$  parallel with the body axis of revolution.

In cases (i)–(ii), one gets  $\nabla \cdot \mathbf{E} = 0$  and also, for an insulating body (Tsinober, 1970), the condition  $\mathbf{j} \cdot \mathbf{n} = 0$  on  $S$  yields the boundary condition  $\mathbf{E} \cdot \mathbf{n} = 0$  on  $S$ . Recalling that  $\nabla \wedge \mathbf{E} = \mathbf{0}$  in the liquid and that  $\mathbf{E}$  vanishes far from the body it follows that  $\mathbf{E} = \mathbf{0}$  in the entire liquid domain. In summary, in cases (i)–(ii) one solely has to determine the flow  $(\mathbf{u}, p)$  by solving steady incompressible Navier–

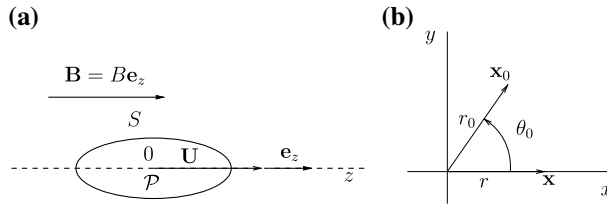


**Figure 1.** (a) A solid body of revolution  $\mathcal{P}$ , with smooth boundary  $S$ , translating at the velocity  $\mathbf{U}$  parallel with its axis of revolution in a quiescent conducting Newtonian liquid in which a uniform magnetic field  $\mathbf{B}$  parallel with  $\mathbf{U}$  prevails. (b) Top view of observation point  $\mathbf{x} = r\mathbf{e}_r + z\mathbf{e}_z$  and source point  $\mathbf{x}_0 = r_0 \cos \theta_0 \mathbf{e}_x + r_0 \sin \theta_0 \mathbf{e}_y + z_0 \mathbf{e}_z$  located on the  $(r - r_0)^2 + (z - z_0)^2 = 0$  ring.

Stokes equations with body force  $\sigma(\mathbf{u} \wedge \mathbf{B}) \wedge \mathbf{B}$ . Without any further assumption on the flow Reynolds number  $Re$  the task remains involved in both cases (i)–(ii) and this explains why quite a few works cope with the subject. Among others one can mention general considerations (Hartmann & Sanchez-Palencia, 1973) for large Hartmann number  $M$  and arbitrary Reynolds number  $Re$  in cases (i)–(ii) and also for moderate Reynolds number the flow about a disk (Yosinobu, 1960; Kalis, Tsinober, Shtern, & Shcherbinin, 1965) in case (i) or about a sphere (Gotoh, 1960) in case (ii).

As soon as  $Re \ll 1$  one can neglect the inertial term in the Navier–Stokes equations therefore ending up with the more tractable linear Stokes equations. This so-called creeping flow model makes it possible to obtain several results in cases (i)–(ii) and for several ranges of the Hartmann number  $M$ : the solution in case (i) for a translating disk with numerical results restricted to  $M \leq \mathcal{O}(1)$  in Yosinobu and Kabutani (1959) and the solution in case (ii) for a sphere and  $M \ll 1$  in Chester (1957) or for an arbitrary body of revolution and  $M \gg 1$  in Chester (1961). In order to efficiently deal with other shapes than a disk in case (i), a new boundary approach has been recently proposed in Sellier, Aydin, and Tezer-Sezgin (2014a). This procedure, which has been found to accurately provide the flow about the body in a large range of Hartmann number, rests on the determination in Sellier, Aydin, and Tezer-Sezgin (2014b) of the associated fundamental MHD two-dimensional plane Stokes flow produced by a concentrated point force with arbitrary strength. In a similar fashion, it would be nice to develop a boundary technique to cope with an arbitrary translating body of revolution in case (ii)! The present work addresses the very first step in this direction, i. e. the derivation of two relevant fundamental axisymmetric MHD Stokes flows due to some axisymmetric distributions of concentrated forces on a ring.

The paper is organised as follows. The governing MHD creeping flow equations in axisymmetric case are given together with the resulting problems for two axisymmetric fundamental flows in Section 2 which also shows how one can build each of the required *axisymmetric* flow from the knowledge of a more complex *three-dimensional* fundamental flow. The determination in closed

form of the three-dimensional and of the two axisymmetric fundamental flows is achieved in Section 3. The numerical implementation together with related accuracy issues are handled in Section 4 which also provides some computed velocity and pressure patterns for each considered axisymmetric fundamental flow. Finally, a few conclusions close the paper in Section 5.

## 2. Governing MHD problems and advocated procedure

This section gives the equations governing the steady creeping MHD axisymmetric flow about a solid body of revolution translating parallel with both its axis of revolution and the ambient uniform magnetic field. It also presents the associated steady axisymmetric MHD Low-Reynolds Number fundamental flows whose determination, which is the matter of the present work, is handled in Section 3.

### 2.1. Governing axisymmetric MHD creeping flow problem and associated fundamental flows

As illustrated in Figure 1(a) and mentioned in the introduction, the problem motivating the present work is the determination of the steady axisymmetric creeping MHD flow about a solid body  $\mathcal{P}$  with axis of revolution  $(O, \mathbf{e}_z)$  translating, without rotating, at a prescribed velocity  $U\mathbf{e}_z$  in a quiescent conducting Newtonian liquid subject to a *uniform* magnetic field  $\mathbf{B} = B\mathbf{e}_z$  with  $B > 0$ .

The liquid has strictly positive uniform viscosity  $\mu$ , density  $\rho$  and conductivity  $\sigma$ , while both the solid body and the liquid have the same uniform magnetic permeability  $\mu_m > 0$ . Designating by  $V = |U| > 0$  the liquid velocity magnitude and by  $a$  the body length scale, the relevant usual Reynolds number  $Re$  and magnetic Reynolds number  $Re_m$  read  $Re = \rho Va/\mu$  and  $Re_m = \mu_m \sigma Va$ , respectively. Assuming that  $Re_m \ll 1$  shows, since the liquid and the body have the same magnetic permeability, that the magnetic field takes the uniform value  $\mathbf{B} = B\mathbf{e}_z$  in the entire liquid domain (Moreau, 1990). Taking  $Re \ll 1$  (i. e. neglecting all inertial effects) also shows that, for our axisymmetric flow, there is no electric field (Tsinober, 1970) in the liquid domain  $\mathcal{D}$ . As a result, the steady creeping flow axisymmetric velocity and pressure fields  $\mathbf{u}$  and  $p$  obey

$$\mu \nabla^2 \mathbf{u} = \nabla p - \sigma B^2 (\mathbf{u} \wedge \mathbf{e}_z) \wedge \mathbf{e}_z \text{ and } \nabla \cdot \mathbf{u} = 0 \text{ in } \mathcal{D}, \quad (2)$$

$$(\mathbf{u}, p) \rightarrow (\mathbf{0}, 0) \text{ as } r = |\mathbf{x}| \rightarrow \infty, \quad (3)$$

$$\mathbf{u} = U\mathbf{e}_z \text{ on } S \quad (4)$$

where  $S$  denotes the body surface.

In dealing with (2)–(4) one can either employ Cartesian coordinates  $O(x, y, z)$  or cylindrical polar coordinates  $(r, \theta, z)$  with  $r = \sqrt{x^2 + y^2} \geq 0, \theta \in [0, 2\pi]$  and  $x = r \cos \theta, y = r \sin \theta$ . Associated unit vectors are the usual triplet  $(\mathbf{e}_x, \mathbf{e}_y, \mathbf{e}_z)$  and the local vectors  $\mathbf{e}_r = \cos \theta \mathbf{e}_x + \sin \theta \mathbf{e}_y$  and  $\mathbf{e}_\theta = \mathbf{e}_z \wedge \mathbf{e}_r$ .

Clearly, the solution to (2)–(4) adopts the general form  $\mathbf{u} = U\mathbf{u}'$  and  $p = \mu U p'/a$  with the normalised flow  $(\mathbf{u}', p')$  solely depending upon the body shape and the Hartmann number  $M$  defined as

$$M = a/d, \quad d := (\sqrt{\mu/\sigma})/B \quad (5)$$

where  $d$  is the so-called Hartmann layer thickness (Hartmann, 1937).

Of course, for a non-conducting liquid (vanishing conductivity  $\sigma$ ) one has  $d \rightarrow \infty (M \rightarrow 0)$  and (2) becomes the usual axisymmetric Stokes equations for which several efficient methods are available (see the standard textbooks (Happel & Brenner, 1983; Kim & Karrila, 1983)). One efficient approach for both fully three-dimensional and axisymmetric Stokes flows is the Boundary Element Method (BEM), thoroughly detailed elsewhere (Pozrikidis, 1992; Sellier, 2006). This powerful technique rests on the determination of the so-called Stokeslet which is the free-space Green's flow of Stokes flow produced by a point force with strength  $\mathbf{g}$  (Happel & Brenner, 1983; Kim & Karrila, 1983; Pozrikidis, 1992). At any point  $\mathbf{x} \neq \mathbf{x}_0$  the Stokeslet velocity  $\mathbf{u}_s(\mathbf{x})$  and pressure  $p_s(\mathbf{x})$  take the very simple forms

$$\mathbf{u}_s(\mathbf{x}) = \frac{1}{8\pi\mu} \left\{ \frac{\mathbf{g}}{|\mathbf{x} - \mathbf{x}_0|} + \frac{[\mathbf{g} \cdot (\mathbf{x} - \mathbf{x}_0)](\mathbf{x} - \mathbf{x}_0)}{|\mathbf{x} - \mathbf{x}_0|^3} \right\}, \quad p_s(\mathbf{x}) = \frac{\mathbf{g} \cdot (\mathbf{x} - \mathbf{x}_0)}{4\pi|\mathbf{x} - \mathbf{x}_0|^3}. \quad (6)$$

The BEM formulation for a Stokes axisymmetric flow is also derived from the fundamental flows produced by a ring of point axial or radial forces (Pozrikidis, 1992).

It should be nice to extend the BEM technique developed for axisymmetric Stokes flows to the present problem (2)–(4) whatever the Hartmann number  $M$ ! A very first step in this direction is the determination of two different fundamental axisymmetric MHD flows produced in the free-space by a prescribed axisymmetric distribution  $\mathbf{F}(\mathbf{x})$  of forces located on the  $r = r_0 > 0$  ring in the  $z = z_0$  plane. Those axisymmetric fundamental flows  $(\mathbf{u}, p)$  obey

$$\mu \nabla^2 \mathbf{u} = \nabla p - \sigma B^2 (\mathbf{u} \wedge \mathbf{e}_z) \wedge \mathbf{e}_z - \mathbf{F} \text{ and } \nabla \cdot \mathbf{u} = 0 \text{ for } r \neq r_0 \text{ and } z \neq z_0, \quad (7)$$

$$(\mathbf{u}, p) \rightarrow (\mathbf{0}, 0) \text{ as } \sqrt{(r - r_0)^2 + (z - z_0)^2} \rightarrow \infty. \quad (8)$$

Denoting by  $\delta$  the usual Dirac one-dimensional pseudo-function, we address in the present paper the following flows:

- (i) A fundamental flow produced by a ring of axial forces with

$$\mathbf{F}(\mathbf{x}) = F \int_0^{2\pi} [\delta(r - r_0)\delta(z - z_0)\delta(\theta - \theta_0)\mathbf{e}_z] d\theta_0 = F\delta(r - r_0)\delta(z - z_0)\mathbf{e}_z \quad (9)$$

(ii) A fundamental flow produced by a ring of radial forces with

$$\mathbf{F}(\mathbf{x}) = F \int_0^{2\pi} [\delta(r - r_0)\delta(z - z_0)\delta(\theta - \theta_0)\mathbf{e}_r(\theta_0)]d\theta_0. \quad (10)$$

The quantity  $F \neq 0$  in (9)–(10) is the given forces strength.

## 2.2. Solution in terms of a three-dimensional fundamental MHD flow

In getting the previous fundamental axisymmetric flows, one can think about two different approaches worked out to derive axisymmetric Green's functions or flows in several fields: acoustics (Dawson, 1995) magnetostatics (Dini, Khorasani & Amrollahi, 2004; Priede & Gerbeth, 2006), elasticity (Kermanidis, 1975; Hasegawa, 1975, 1976, 1981, 1984, 1988, 1992), Stokes flow (Pozrikidis, 1992) and MHD viscous flow (Tsinober, 1973; Tsinober, 1973; Priede, 2013). In those works two procedures are employed: the direct treatment of the axisymmetric Green's problem using a Bessel transformation in Dini, Khorasani & Amrollahi (2004), Hasegawa (1975, 1976, 1981, 1984, 1988, 1992) or, for the other previously quoted references, the integration over a ring of given distributions of *three-dimensional* Green's function (or flow). In the present paper, it has been found more tractable to use the second three-dimensional Green's flow approach.

Accordingly, we look at the *three-dimensional* fundamental MHD viscous flow produced, in the entire space where prevails the uniform magnetic field  $\mathbf{B} = B\mathbf{e}_z$ , by a concentrated point source with arbitrary strength  $\mathbf{g}$  located at point  $\mathbf{x}_0$ . Since fully three-dimensional, this flow with velocity  $\mathbf{v}$  and pressure  $q$  induces a steady electric field  $\mathbf{E} = -\nabla\phi$  with  $\phi$  the electric potential. Imposing the charge conservation  $\nabla \cdot \mathbf{j} = 0$  and recalling the Ohm's law for the current density  $\mathbf{j}$ , one arrives at the fundamental basic three-dimensional problem

$$\mu\nabla^2\mathbf{v} = \nabla q + \sigma B\nabla\phi \wedge \mathbf{e}_z - \sigma B^2(\mathbf{v} \wedge \mathbf{e}_z) \wedge \mathbf{e}_z - \delta(\mathbf{x} - \mathbf{x}_0)\mathbf{g} \text{ for } \mathbf{x} \neq \mathbf{x}_0, \quad (11)$$

$$\nabla \cdot \mathbf{v} = 0 \text{ and } \Delta\phi = B\nabla \cdot (\mathbf{v} \wedge \mathbf{e}_z) \text{ for } \mathbf{x} \neq \mathbf{x}_0, \quad (12)$$

$$(\mathbf{v}, q, \nabla\phi) \rightarrow (\mathbf{0}, 0, \mathbf{0}) \text{ as } |\mathbf{x} - \mathbf{x}_0| \rightarrow \infty \quad (13)$$

with  $\Delta$  and  $\delta$  the three-dimensional Laplacian operator and Dirac delta pseudo-function, respectively.

By linearity, it turns out that at each point  $\mathbf{x} \neq \mathbf{x}_0$  the fundamental flow reads

$$\mu\mathbf{v}(\mathbf{x}) = \mathbf{V}(x - x_0, y - y_0, z - z_0) \cdot \mathbf{g}, \quad q(\mathbf{x}) = \mathbf{Q}(x - x_0, y - y_0, z - z_0) \cdot \mathbf{g} \quad (14)$$

where the Cartesian components of the second-rank velocity Green tensor  $\mathbf{V}$  and Green pressure vector  $\mathbf{Q}$  will be obtained in Section 3.1. From those Cartesian components, we then build the two required fundamental axisymmetric MHD flows  $(\mathbf{u}, p)$ , solution to (7)–(8) with force distributions  $\mathbf{F}$  given by (9)–(10), by spreading source points  $\mathbf{x}_0$  on the entire  $(z - z_0)^2 + (r - r_0)^2 = 0$  ring. Under

our notations, each resulting axisymmetric flow  $(\mathbf{u}, p)$  reads, at point  $\mathbf{x}(r, \theta, z)$ ,

$$\mathbf{u}(\mathbf{x}) = u_r(r, z)\mathbf{e}_r + u_z(r, z)\mathbf{e}_\theta, \quad p(\mathbf{x}) = p(r, z) \quad (15)$$

and, as illustrated in Figure 1(b), it is thus sufficient to get  $(u_r, u_z, p)$  at the point  $\mathbf{x} = r\mathbf{e}_x + z\mathbf{e}_z$  taking for each point  $\mathbf{x}_0$  located on the ring cylindrical coordinates  $(r_0, \theta_0, z_0)$  with  $\theta_0 \in [0, 2\pi]$ .

Under this choice  $x = r, y = 0, x_0 = r_0 \cos \theta_0$  and  $y_0 = r_0 \sin \theta_0$ . Recalling the relations (14) and the definitions (9)–(10), the first axisymmetric fundamental flow produced by the ring of axial forces (9) then readily writes

$$\mu u_r(r, z) = F \int_0^{2\pi} V_{xz}(r - r_0 \cos \theta_0, -r_0 \sin \theta_0, z - z_0) d\theta_0, \quad (16)$$

$$\mu u_z(r, z) = F \int_0^{2\pi} V_{zz}(r - r_0 \cos \theta_0, -r_0 \sin \theta_0, z - z_0) d\theta_0, \quad (17)$$

$$p(r, z) = F \int_0^{2\pi} Q_z(r - r_0 \cos \theta_0, -r_0 \sin \theta_0, z - z_0) d\theta_0 \quad (18)$$

while because  $\mathbf{e}_r(\theta_0) = \cos \theta_0 \mathbf{e}_x + \sin \theta_0 \mathbf{e}_y$ , the second axisymmetric fundamental flow induced by the ring of radial forces (10) is this time given by

$$\begin{aligned} \mu u_r(r, z) = F \int_0^{2\pi} \{ & \cos \theta_0 V_{xx}(r - r_0 \cos \theta_0, -r_0 \sin \theta_0, z - z_0) \\ & + \sin \theta_0 V_{xy}(r - r_0 \cos \theta_0, -r_0 \sin \theta_0, z - z_0) \} d\theta_0, \end{aligned} \quad (19)$$

$$\begin{aligned} \mu u_z(r, z) = F \int_0^{2\pi} \{ & \cos \theta_0 V_{zx}(r - r_0 \cos \theta_0, -r_0 \sin \theta_0, z - z_0) \\ & + \sin \theta_0 V_{zy}(r - r_0 \cos \theta_0, -r_0 \sin \theta_0, z - z_0) \} d\theta_0, \end{aligned} \quad (20)$$

$$\begin{aligned} p(r, z) = F \int_0^{2\pi} \{ & \cos \theta_0 Q_x(r - r_0 \cos \theta_0, -r_0 \sin \theta_0, z - z_0) \\ & + \sin \theta_0 Q_y(r - r_0 \cos \theta_0, -r_0 \sin \theta_0, z - z_0) \} d\theta_0. \end{aligned} \quad (21)$$

In summary, the results (16)–(21) express the two required fundamental flows in terms of the vector  $\mathbf{Q}$  and of only six Cartesian components of the second-rank tensor  $\mathbf{V}$ .

### 3. Determination of each addressed fundamental flow

As shown in Section 2.2, the task consists in determining the fundamental three-dimensional viscous MHD flow  $(\mathbf{v}, q)$  governed by (11)–(13). The needed Cartesian components of the associated tensor  $\mathbf{V}$  and vector  $\mathbf{Q}$  (see (14)) are obtained in Section 3.1 while the axisymmetric fundamental flows are deduced in Section 3.2 and Section 3.3.

### 3.1. Fundamental three-dimensional viscous MHD flow

#### 3.1.1. Analytical solution

Clearly, there is no need for the present work to gain the electric potential  $\phi$  coupled to the required flow  $(\mathbf{v}, q)$  through the second equation (12). Since the derivation of  $(\mathbf{v}, q)$  has been nicely achieved in [Priede \(2013\)](#), we briefly give below the required steps. First, we get rid of the pressure  $q$  by applying the operator  $\nabla \wedge (\nabla \wedge )$  to (11). Taking into account both relations (12) then easily yields

$$\mu \nabla^2 (\nabla^2 \mathbf{v}) - \sigma B^2 \frac{\partial^2 \mathbf{v}}{\partial z^2} = \nabla \wedge (\nabla \wedge [\delta \mathbf{g}]). \quad (22)$$

Recalling the definition (5) of the Hartmann layer thickness  $d$  and because  $\mathbf{g}$  is constant the required velocity  $\mathbf{v}$  is thus given by

$$\mu \mathbf{v} = \nabla \wedge (\nabla \wedge [H \mathbf{g}]), \quad \Delta (\Delta H) - \frac{1}{d^2} \frac{\partial^2 H}{\partial z^2} = \delta (\mathbf{x} - \mathbf{x}_0). \quad (23)$$

Upon introducing, for a vector field  $\mathbf{a}$ , the linear operator  $L$  as

$$L[\mathbf{a}] = \Delta (\nabla \cdot \mathbf{a}) - \frac{1}{d^2} \frac{\partial}{\partial z} (\mathbf{a} \cdot \mathbf{e}_z) \quad (24)$$

and applying this operator to (11) now gives, exploiting (12), a governing equation for the pressure  $q$ . This equation is

$$\Delta (\Delta q) - \frac{1}{d^2} \frac{\partial^2 q}{\partial z^2} = L[\delta \mathbf{g}]. \quad (25)$$

By virtue of the governing equation (23) for the function  $H$ , it follows that

$$q = L[H \mathbf{g}] = \Delta [\nabla \cdot (H \mathbf{g})] - \frac{1}{d^2} \frac{\partial}{\partial z} [H (\mathbf{g} \cdot \mathbf{e}_z)]. \quad (26)$$

As required by (13) and shown by (23) and (26), it is thus sufficient to obtain the function  $H$  solution to the second identity (23) and such that both  $\mathbf{v}$  and  $q$  vanish as  $|\mathbf{x} - \mathbf{x}_0| \rightarrow \infty$ . Clearly  $H$  is thus defined up to a constant. In this paper, we select a solution  $H$  by adding a constant to the one proposed in [Priede \(2013\)](#). The retained solution is

$$H(\mathbf{x}, \mathbf{x}_0) = -\frac{d}{8\pi} \left\{ E_1 \left( \frac{|\mathbf{x} - \mathbf{x}_0| - (z - z_0)}{2d} \right) + E_1 \left( \frac{|\mathbf{x} - \mathbf{x}_0| + (z - z_0)}{2d} \right) + 2 \log \left( \frac{\sqrt{(x - x_0)^2 + (y - y_0)^2}}{2d} \right) + 2\gamma \right\} \quad (27)$$

where  $\gamma$  denotes the usual Euler's constant and  $E_1$  is the exponential integral function defined [Abramowitz and Stegun \(1965\)](#) as  $E_1(t) = \int_t^\infty s^{-1} e^{-s} ds$  for  $t > 0$ ,

In summary, the fundamental three-dimensional flow  $(\mathbf{v}, q)$  is obtained from (23) and (26)–(27). This analytical solution suggests the following remarks:

- (i) As consistent with the announced relations (14), note that  $H = H(\mathbf{x} - \mathbf{x}_0)$ .
- (ii) As  $t \rightarrow 0^+$  one has  $E_1(t) \sim -\gamma - \log t + t + \mathcal{O}(t^2)$  (see Abramowitz & Stegun, 1965). Accordingly, the following basic asymptotics hold

$$H(\mathbf{x}, \mathbf{x}_0) \sim H_s(|\mathbf{x} - \mathbf{x}_0|) \text{ as } |\mathbf{x} - \mathbf{x}_0| \rightarrow 0 \text{ or as } d \rightarrow \infty, \quad H_s(t) = -t/(8\pi). \quad (28)$$

Not surprisingly, the above function  $H_s$  is the one obtained for the Stokes flow (see the derivation of the Stokeslet solution in Pozrikidis (1992)). As the reader may check, putting  $H_s$  into (23) and (26) indeed produces as fundamental flow  $(\mathbf{v}, p)$  the Stokeslet solution (6).

- (iii) It is worth pointing out the useful relations below (which may be either directly retrieved by the reader from (27) or deduced, for (29)–(30), from Priede (2013))

$$-4\pi \Delta H = \cosh\left(\frac{z - z_0}{2d}\right) \frac{e^{-|\mathbf{x} - \mathbf{x}_0|/(2d)}}{|\mathbf{x} - \mathbf{x}_0|}, \quad (29)$$

$$-4\pi \frac{\partial H}{\partial z} = d \sinh\left(\frac{z - z_0}{2d}\right) \frac{e^{-|\mathbf{x} - \mathbf{x}_0|/(2d)}}{|\mathbf{x} - \mathbf{x}_0|}, \quad (30)$$

$$-8\pi \frac{\partial H}{\partial x} = d(x - x_0) \left\{ \frac{2}{(x - x_0)^2 + (y - y_0)^2} - \frac{e^{-|\mathbf{x} - \mathbf{x}_0|/(2d)}}{|\mathbf{x} - \mathbf{x}_0|} \left[ \frac{e^{(z - z_0)/(2d)}}{|\mathbf{x} - \mathbf{x}_0| - (z - z_0)} + \frac{e^{-(z - z_0)/(2d)}}{|\mathbf{x} - \mathbf{x}_0| + z - z_0} \right] \right\}. \quad (31)$$

Those relations will be of interest in Section 3.1.2.

### 3.1.2. Resulting required vector $\mathbf{Q}$ and Cartesian components of tensor $\mathbf{V}$

The resulting Cartesian components of the second-rank velocity tensor  $\mathbf{V}$  and pressure vector  $\mathbf{Q}$  have not been given in Priede (2013). Those needed quantities are here calculated from the previous results (23), (26)–(27) and (29)–(31).

Taking first  $\mathbf{g} = \mathbf{e}_z$  immediately provides the relations

$$V_{xz} = \frac{\partial^2 H}{\partial x \partial z}, \quad V_{zz} = \frac{\partial^2 H}{\partial z^2} - \Delta H, \quad Q_z = \frac{\partial \Delta H}{\partial z} - \frac{1}{d^2} \frac{\partial H}{\partial z}. \quad (32)$$

Setting henceforth  $R = |\mathbf{x} - \mathbf{x}_0|$  it follows from (29)–(30) that (anticipating on the equality  $V_{zx} = V_{xz}$  obtained for  $\mathbf{g} = \mathbf{e}_x$ )

$$V_{xz} = V_{zx} = \sinh\left(\frac{z - z_0}{2d}\right) \left[ 1 + \frac{2d}{R} \right] \left[ \frac{x - x_0}{R} \right] \frac{e^{-R/(2d)}}{8\pi R}, \quad (33)$$

$$V_{zz} = \left\{ \cosh\left(\frac{z - z_0}{2d}\right) + \sinh\left(\frac{z - z_0}{2d}\right) \left[ 1 + \frac{2d}{R} \right] \left[ \frac{z - z_0}{R} \right] \right\} \frac{e^{-R/(2d)}}{8\pi R}, \quad (34)$$

$$Q_z = \left(\frac{1}{d}\right) \left\{ \sinh\left(\frac{z-z_0}{2d}\right) + \cosh\left(\frac{z-z_0}{2d}\right) \left[1 + \frac{2d}{R}\right] \left[\frac{z-z_0}{R}\right] \right\} \frac{e^{-R/(2d)}}{8\pi R}. \quad (35)$$

Selecting now  $\mathbf{g} = \mathbf{e}_x$  or  $\mathbf{g} = \mathbf{e}_y$  yields the announced identity  $V_{xz} = V_{zx}$  and

$$V_{xx} = \frac{\partial^2 H}{\partial x^2} - \Delta H, \quad V_{xy} = \frac{\partial^2 H}{\partial y \partial x}, \quad V_{zy} = \frac{\partial^2 H}{\partial y \partial z}, \quad Q_x = \frac{\partial \Delta H}{\partial x}, \quad Q_y = \frac{\partial \Delta H}{\partial y}. \quad (36)$$

Accordingly, from (29)–(30), one gets

$$V_{zy} = \sinh\left(\frac{z-z_0}{2d}\right) \left[1 + \frac{2d}{R}\right] \left[\frac{y-y_0}{R}\right] \frac{e^{-R/(2d)}}{8\pi R}, \quad (37)$$

$$Q_x = \left(\frac{1}{d}\right) \cosh\left(\frac{z-z_0}{2d}\right) \left[1 + \frac{2d}{R}\right] \left[\frac{x-x_0}{R}\right] \frac{e^{-R/(2d)}}{8\pi R}, \quad (38)$$

$$Q_y = \left(\frac{1}{d}\right) \cosh\left(\frac{z-z_0}{2d}\right) \left[1 + \frac{2d}{R}\right] \left[\frac{y-y_0}{R}\right] \frac{e^{-R/(2d)}}{8\pi R}. \quad (39)$$

In a similar fashion, using again (29) but also this time (31) for  $\partial H/\partial x$ , provides after more (although elementary) manipulations the desired quantities  $V_{xx}$  and  $V_{xy}$ . It is finally found that

$$V_{xx} = \frac{1}{8\pi} \left\{ 2 \cosh\left(\frac{z-z_0}{2d}\right) g(R, d) + d [T_1 - (x-x_0)^2 T_2] \right\}, \quad (40)$$

$$V_{xy} = - \left[ \frac{d(x-x_0)(y-y_0)}{8\pi} \right] T_2 \quad (41)$$

with functions  $T_1$  and  $T_2$ , depending upon  $(R, z-z_0, d)$ , defined in Appendix 1.

### 3.2. Fundamental flow produced by an axial force distribution

For this flow we employ (16)–(18) in conjunction with (33)–(35) in which we use the relations (recall Section 2.2 and Figure 1(b))  $x = r, y = 0, x_0 = r_0 \cos \theta_0$  and  $y_0 = r_0 \sin \theta_0$ . Moreover, we have the basic identity and useful definition (see Appendix 1)

$$R = \{r^2 + r_0^2 - 2rr_0 \cos \theta_0 + (z-z_0)^2\}^{1/2}, \quad g(R, d) = e^{-R/(2d)}/R. \quad (42)$$

Under those notations, it follows that

$$8\pi \mu u_r(r, z) = F \sinh\left(\frac{z-z_0}{2d}\right) \int_0^{2\pi} \left[\frac{g(R, d)}{R}\right] \left[1 + \frac{2d}{R}\right] (r - r_0 \cos \theta_0) d\theta_0, \quad (43)$$

$$8\pi \mu u_z(r, z) = F \cosh\left(\frac{z-z_0}{2d}\right) \int_0^{2\pi} g(R, d) d\theta_0$$

$$+ F(z - z_0) \sinh\left(\frac{z - z_0}{2d}\right) \int_0^{2\pi} \left[\frac{g(R, d)}{R}\right] \left[1 + \frac{2d}{R}\right] d\theta_0, \quad (44)$$

$$\begin{aligned} 8\pi dp(r, z) &= F \sinh\left(\frac{z - z_0}{2d}\right) \int_0^{2\pi} g(R, d) d\theta_0 \\ &+ F(z - z_0) \cosh\left(\frac{z - z_0}{2d}\right) \int_0^{2\pi} \left[\frac{g(R, d)}{R}\right] \left[1 + \frac{2d}{R}\right] d\theta_0. \end{aligned} \quad (45)$$

As  $d \rightarrow \infty$  one retrieves the fundamental Stokes flow given in [Pozrikidis \(1992\)](#).

### 3.3. Fundamental flow produced by a radial force distribution

For this second flow, we appeal this time to (19)–(21) and arrive at the following velocity components and pressure

$$\begin{aligned} 8\pi \mu u_r(r, z) &= 2F \cosh\left(\frac{z - z_0}{2d}\right) \int_0^{2\pi} g(R, d) \cos \theta_0 d\theta_0, \\ &+ Fd \int_0^{2\pi} \left\{ T_1 \cos \theta_0 - (r - r_0 \cos \theta_0)(r \cos \theta_0 - r_0) T_2 \right\} d\theta_0, \end{aligned} \quad (46)$$

$$8\pi \mu u_z(r, z) = F \sinh\left(\frac{z - z_0}{2d}\right) \int_0^{2\pi} \left[\frac{g(R, d)}{R}\right] \left[1 + \frac{2d}{R}\right] (r \cos \theta_0 - r_0) d\theta_0, \quad (47)$$

$$8\pi dp(r, z) = F \cosh\left(\frac{z - z_0}{2d}\right) \int_0^{2\pi} \left[\frac{g(R, d)}{R}\right] \left[1 + \frac{2d}{R}\right] (r \cos \theta_0 - r_0) d\theta_0. \quad (48)$$

Clearly, the more complicated quantity is the radial velocity component  $u_r$  since it involves both non-trivial functions  $T_1$  and  $T_2$  displayed in [Appendix 1](#). Again, the limit of (46)–(48) as  $d \rightarrow \infty$  recovers the associated fundamental Stokes flow discussed in [Pozrikidis \(1992\)](#).

## 4. Numerical method and flow patterns

From [Section 3.2](#) and [Section 3.3](#), we can restrict attention to the case  $z_0 = 0$ . This section is devoted to the numerical implementation of the previous results (43)–(48) for  $z_0 = 0$ . It permits us to plot, in normalised coordinates  $\bar{r} = r/d$  and  $\bar{z} = z/d$ , the resulting flow patterns for a few values of the normalised ring radius  $\bar{r}_0 = r_0/d > 0$ .

### 4.1. Numerical implementation and accuracy issues

For given liquid viscosity  $\mu$  and conductivity  $\sigma$  imposing the uniform ambient magnetic field  $\mathbf{B} = B\mathbf{e}_z$  actually prescribes the Hartmann layer thickness

$d = (\sqrt{\mu/\sigma})/B > 0$ . Henceforth, we set  $z_0 = 0$  and use normalised coordinates  $\bar{r} = r/d$  and  $\bar{z} = z/d$ . The normalised distance  $\bar{R} = R/d$  is given by (setting  $z_0 = 0$  in (42))

$$\bar{R} = \{\bar{r}^2 + \bar{r}_0^2 - 2\bar{r}\bar{r}_0 \cos \theta_0 + \bar{z}^2\}^{1/2}. \quad (49)$$

Inspecting (43)–(48) suggests introducing seven integrals  $J_{10}, J_{20}, J_{30}, J_{11}, J_{21}, J_{31}$  and  $J$  defined as

$$J_{mn} = \int_0^{2\pi} [\bar{R}]^{-m} e^{-\bar{R}/2} \cos^n \theta_0 d\theta_0 \text{ for } n = 0, 1 \text{ and } m = 1, 2, 3, \quad (50)$$

$$J = \int_0^{2\pi} \{\bar{T}_1 \cos \theta_0 - (\bar{r} - \bar{r}_0 \cos \theta_0)(\bar{r} \cos \theta_0 - \bar{r}_0)\bar{T}_2\} d\theta_0 \quad (51)$$

with occurring functions  $\bar{T}_1$  and  $\bar{T}_2$  obtained by replacing  $(R, z, z_0, d)$  with  $(\bar{R}, \bar{z}, 0, 1)$  in (A2)–(A3) and given in Appendix 3. Under those notations one obtains:

(i) For the axial force distribution (using (43)–(45)), the associated first fundamental flow  $(u_r^{(1)}, u_z^{(1)}, p^{(1)})$  is given by

$$8\pi \mu du_r^{(1)}/F = \sinh\left(\frac{\bar{z}}{2}\right) \{(J_{20} + 2J_{30})\bar{r} - (J_{21} + 2J_{31})\bar{r}_0\}, \quad (52)$$

$$8\pi \mu du_z^{(1)}/F = \cosh\left(\frac{\bar{z}}{2}\right) J_{10} + \bar{z} \sinh\left(\frac{\bar{z}}{2}\right) (J_{20} + 2J_{30}), \quad (53)$$

$$8\pi d^2 p^{(1)}/F = \sinh\left(\frac{\bar{z}}{2}\right) J_{10} + \bar{z} \cosh\left(\frac{\bar{z}}{2}\right) (J_{20} + 2J_{30}). \quad (54)$$

(ii) For the radial force distribution (using this time (46)–(48)) the second fundamental flow  $(u_r^{(2)}, u_z^{(2)}, p^{(2)})$  satisfies

$$8\pi \mu du_r^{(2)}/F = 2 \cosh\left(\frac{\bar{z}}{2}\right) J_{11} + J, \quad (55)$$

$$8\pi \mu du_z^{(2)}/F = \sinh\left(\frac{\bar{z}}{2}\right) \{(J_{21} + 2J_{31})\bar{r} - (J_{20} + 2J_{30})\bar{r}_0\}, \quad (56)$$

$$8\pi d^2 p^{(2)}/F = \cosh\left(\frac{\bar{z}}{2}\right) \{(J_{21} + 2J_{31})\bar{r} - (J_{20} + 2J_{30})\bar{r}_0\}. \quad (57)$$

In view (52)–(57), calculating the flows  $(u_r^{(l)}, u_z^{(l)}, p^{(l)})$  (with  $l = 1, 2$ ) in the half  $\bar{z} - \bar{r}$  plane ( $\bar{r} \geq 0$ ), outside the point  $(\bar{r} - \bar{r}_0)^2 + \bar{z}^2 = 0$  (which is the ring trace), requires to compute the integrals  $J_{mn}$  and  $J$ . Those integrals solely depend upon  $(\bar{r}_0, \bar{r}, \bar{z})$  and are strongly sensitive to the distant  $\bar{h} = [(\bar{r} - \bar{r}_0)^2 + \bar{z}^2]^{1/2} > 0$ .

We first pay attention to the integrals  $J_{mn}$ . It is found that for a sufficiently distant point ( $\bar{h} \geq \mathcal{O}(1)$ ) usual quadratures with a few Gaussian points ensures a good accuracy even for  $\bar{h}$  large (a case for which putting the  $\sinh(\bar{z}/2)$  or  $\cosh(\bar{z}/2)$  factors inside the integrations over  $\theta_0$  yields the same results). For a point located close the ring ( $0 < \bar{h} = o(1)$ ) much more Gaussian points

are needed because each integral now approaches a weakly singular one. To examine to which extent a good accuracy is reached without any special care, a 'regularization' technique has also been employed to evaluate each integral  $J_{mn}$ . In this approach,  $J_{mn}$  is splitted into a regularised integral and some other terms involving the integrals  $I_{mn}$  defined as

$$I_{mn} = \int_0^{2\pi} [\bar{R}]^{-m} \cos^n \theta_0 d\theta_0 \text{ for } n = 0, 1 \text{ and } m = 1, 2, 3. \quad (58)$$

The integrals  $I_{mn}$  have been actually previously encountered for the axisymmetric Stokes fundamental flows (see, for instance, (Pozrikidis, 1992)). Here, we adopt for small  $\bar{h}$  and  $n = 0, 1$  the decompositions

$$J_{1n} = \int_0^{2\pi} [\bar{R}]^{-1} \left[ e^{-\bar{R}/2} - 1 \right] \cos^n \theta_0 d\theta_0 + I_{1n}, \quad (59)$$

$$J_{2n} = \int_0^{2\pi} [\bar{R}]^{-2} \left[ e^{-\bar{R}/2} - 1 + \bar{R}/2 \right] \cos^n \theta_0 d\theta_0 + I_{2n} - I_{1n}/2, \quad (60)$$

$$J_{3n} = \int_0^{2\pi} [\bar{R}]^{-3} \left[ e^{-\bar{R}/2} - 1 + \bar{R}/2 - \bar{R}^2/8 \right] \cos^n \theta_0 d\theta_0 + I_{3n} - I_{2n}/2 + I_{1n}/8. \quad (61)$$

Clearly, the first integral on the right-hand side of each above decomposition is regular even for vanishing  $\bar{h}$ .

As detailed in Pozrikidis (1992), the accurate determination of the integrals  $I_{mn}$  is done by expressing each integral in terms of the usual complete elliptic integrals of the first and second kind  $F$  and  $E$  (Gradshteyn & Ryzhik, 1965). Those latter integrals are defined for  $0 \leq t < 1$  as

$$F(t) = \int_0^{\pi/2} (1 - t^2 \sin^2 \omega)^{-1/2} d\omega, \quad E(t) = \int_0^{\pi/2} (1 - t^2 \sin^2 \omega)^{1/2} d\omega. \quad (62)$$

Setting  $\theta_0 = \pi - 2\omega$  indeed yields the relations

$$I_{mn} = \frac{4k^m}{(4\bar{r}\bar{r}_0)^{m/2}} \int_0^{\pi/2} \frac{(2 \sin^2 \omega - 1) d\omega}{(1 - k^2 \sin^2 \omega)^{n/2}}, \quad k = \left[ \frac{4\bar{r}\bar{r}_0}{(\bar{r} + \bar{r}_0)^2 + \bar{z}^2} \right]^{1/2} \quad (63)$$

which make it possible to write, as displayed in Appendix 2, each integral  $I_{mn}$  solely in terms of  $\bar{r}, \bar{r}_0, k$  and the elliptic integrals  $F(k)$  and  $E(k)$  which are here computed by calling Fortran subroutines.

We compared the ability, in terms of number of Gaussian points and accuracy, of the direct and regularised methods. The results are illustrated by giving in Table 1, for  $\bar{r}_0 = 1$ , the computed integrals  $J_{m0}$  at three points located in the  $\bar{z} - \bar{r}$  plane in the vicinity of the ring trace:  $P_1(0, 1 + \bar{h})$ ,  $P_2(0, 1 - \bar{h})$  and  $P_3(\bar{h}, 1)$ . The table considers the demanding value  $\bar{h} = 0.001$  and indicates the number  $N$  of Gaussian points used for the direct integration over  $[0, 2\pi]$  (Method 1), the direct

**Table 1.** Computed integrals  $J_{10}$ ,  $J_{20}$  and  $J_{30}$  at points  $P_1$ ,  $P_2$  and  $P_3$  located very close the ring trace ( $\bar{h} = 0.001$ ) in the  $\bar{z} - \bar{r}$  plane using either direct or regularisation methods ( $M = m$  for Method  $m$ ).

P	M	N	$J_{10}$	$J_{20}$	$J_{30}$
$P_1$	1	1024	15.61037048265319	3131.686002842942	1997434.739654201
$P_1$	2	512	15.61037048282996	3131.686003112822	1997434.739990571
$P_1$	3	256	15.61037048288568	3131.68600288449	1997434.740055039
$P_1$	4		15.61037048286234	3131.686003166309	1997434.740054467
$P_2$	1	1024	15.62573470565284	3134.819724575156	1999433.177987192
$P_2$	2	512	15.62573470492680	3134.819723404632	1999433.176471672
$P_2$	3	128	15.62573470493114	3134.819723417441	1999433.177855004
$P_2$	4		15.62573470559920	3134.819724480102	1999433.177854478
$P_3$	1	1024	15.61804696551391	3133.251688551726	1998433.209514288
$P_3$	2	512	15.61804696531082	3133.251688237248	1998433.209117909
$P_3$	3	128	15.61804696530070	3133.251688392196	1998433.209539091
$P_3$	4		15.61804696553471	3133.251688576636	1998433.209539000

**Table 2.** Computed integrals  $J_{11}$ ,  $J_{21}$  and  $J_{31}$  at points  $P_1$ ,  $P_2$  and  $P_3$  located very close the ring trace ( $\bar{h} = 0.001$ ) in the  $\bar{z} - \bar{r}$  plane using either direct or regularisation methods ( $M = m$  for Method  $m$ ).

P	M	N	$J_{11}$	$J_{21}$	$J_{31}$
$P_1$	1	1024	13.73818993760090	3129.9436129152341	1997427.939985994
$P_1$	2	512	13.73818993777768	3129.943613185113	1997427.940322366
$P_1$	3	128	13.73818993777768	3129.943613185113	1997427.940322366
$P_1$	4		13.73818993781008	3129.943613238599	1997427.940386263
$P_2$	1	1024	13.75031422679633	3133.072910110099	1999426.358016457
$P_2$	2	512	13.75031422607029	3133.072908939588	1999426.356500937
$P_2$	3	128	13.75031422607465	3133.072908952396	1999426.356530830
$P_2$	4		13.75031422674271	3133.072910015055	1999426.357883743
$P_3$	1	1024	13.74424780775037	3131.507088769532	1998426.399707410
$P_3$	2	512	13.74424780754728	3131.507088455040	1998426.399311033
$P_3$	3	128	13.74424780753714	3131.507088609985	1998426.399497232
$P_3$	4		13.74424780777115	3131.507088794434	1998426.399732121

integration over  $[0, \pi/2]$  using symmetries and the variable  $\nu = \theta_0/2$  (Method 2) and the direct integration (again over  $[0, \pi/2]$ ) of the regularised integrals arising in (59)–(61) (Method 3). The reported values, obtained using a Fortran double precision Code, have also been compared against a direct integration over  $[0, 2\pi]$  by the Mathematica Software (Method 4) which performs an optimum and adaptive numerical integration method instead of the standard Gaussian procedure (consequently, no number of Gaussian is given for Method 4).

Inspecting Table 1 shows that all methods perfectly agree. As expected, the ‘regularization’ technique requires fewer Gaussian points than the others methods. A similar behaviour is also observed in Table 2 for the other integrals  $J_{m1}$  evaluated at the same points  $P_1$ ,  $P_2$  and  $P_3$ . Accordingly, the ‘regularization’ procedure is well adapted to compute each flow in the vicinity of the ring.

In summary, it has thus been found both efficient and accurate to resort to the ‘regularization’ technique to evaluate the integrals  $J_{mn}$  close to the ring while away from the ring a direct integration is fine. Moreover, when  $\bar{h}$  becomes large it appeared convenient for accuracy reasons to put the  $\sinh(\bar{z}/2)$  or  $\cosh(\bar{z}/2)$

**Table 3.** Computed integral  $J$  for  $\bar{r} = \bar{r}_0 = 1$  and several positive values of  $\bar{z}$  using or not the alternative form (see Appendix 3) for  $\bar{T}_1$  and/or  $\bar{T}_2$ . In the concerned columns we indicate each term for which the alternative form has been employed.

$\bar{z}$	None	$\bar{T}_1$	$\bar{T}_2$	$\bar{T}_1, \bar{T}_2$	Mathematica
1	-0.3716369059	-0.3715230691	-0.3716369059	-0.3715230691	-0.3715230691
5	2897.1184627	-0.0291278082	2897.1184627	-0.0291278082	-0.0291278082
10	11706.606402	-0.0036452547	11706.606402	-0.0036452547	-0.0036452547

**Table 4.** Computed integral  $J$  at points  $P_1, P_2$  and  $P_3$  located very close the ring trace ( $\bar{h} = 0.001$ ) in the  $\bar{z} - \bar{r}$  plane using different methods (with or without the alternative form for  $\bar{T}_1$  and/or  $\bar{T}_2$ ).

Method	$P_1$	$P_2$	$P_3$
None	13.73818993771359	13.75031422468661	11.74160727094769
$\bar{T}_1$	13.73818993771365	13.75031422468683	11.74425728885313
$\bar{T}_2$	13.73818993771342	13.75031422468666	11.74160727094769
$\bar{T}_1, \bar{T}_2$	13.73818993771349	13.75031422468688	11.74425728885313
Mathematica	13.73818993781008	13.75031422674270	11.74425728919264

factors (see (52)–(57)) in the integrals before performing such a direct integration.

The last integral  $J$ , defined by (51), also writes (set  $\alpha = \theta_0/2$ )

$$J = 4 \int_0^{\pi/2} \left\{ \bar{T}_1 - (\bar{r} - \bar{r}_0 \cos 2\alpha)(\bar{r} \cos 2\alpha - \bar{r}_0) \bar{T}_2 \right\} d\alpha. \quad (64)$$

It turns out that computing  $J$  (again in Fortran) with a Gaussian quadrature using the definitions (A2)–(A3) experiences troubles on the  $\bar{r} = \bar{r}_0$  tube far enough from the ring! This difficulty is illustrated in Table 3 (compare the second and last columns) for  $\bar{r}_0 = 1$  and  $\bar{z} = 1, 5, 10$ .

The problem is due to the last terms on the right-hand sides of (A2) and (A3) because  $\bar{R}^2 - \bar{z}^2 = 2\bar{r}^2(1 - \cos 2\alpha)$  vanishes at  $\alpha = 0$  although both  $\bar{T}_1$  and  $(1 - \cos 2\alpha)^2 \bar{T}_2$  admit a finite limit. To circumvent this numerical Problem, we recast  $\bar{T}_1$  and  $\bar{T}_2$  into equivalent alternative forms depending upon the sign of  $\bar{z}$  and displayed in Appendix 3. As seen in Table 3 for  $\bar{z} > 0$ , the use of those alternative forms nicely solves the previous accuracy troubles.

As for the integrals  $J_{mn}$  comparisons at previous points  $P_1, P_2$  and  $P_3$  located near the ring trace have been made for the integral  $J$  using or not the alternative forms for  $\bar{T}_1$  and/or  $\bar{T}_2$ . The obtained results for  $\bar{r}_0 = 1$  and  $\bar{h}_0 = 0.001$  are presented in Table 4. It turns out that it is not necessary to use the alternative forms for  $\bar{h}$  small.

## 4.2. Flow patterns

We now turn to the different fundamental flow patterns for a few values of ring normalised radius  $\bar{r}_0$ . More precisely, we plot in the  $\bar{z} - \bar{r}$  half plane the isolevel

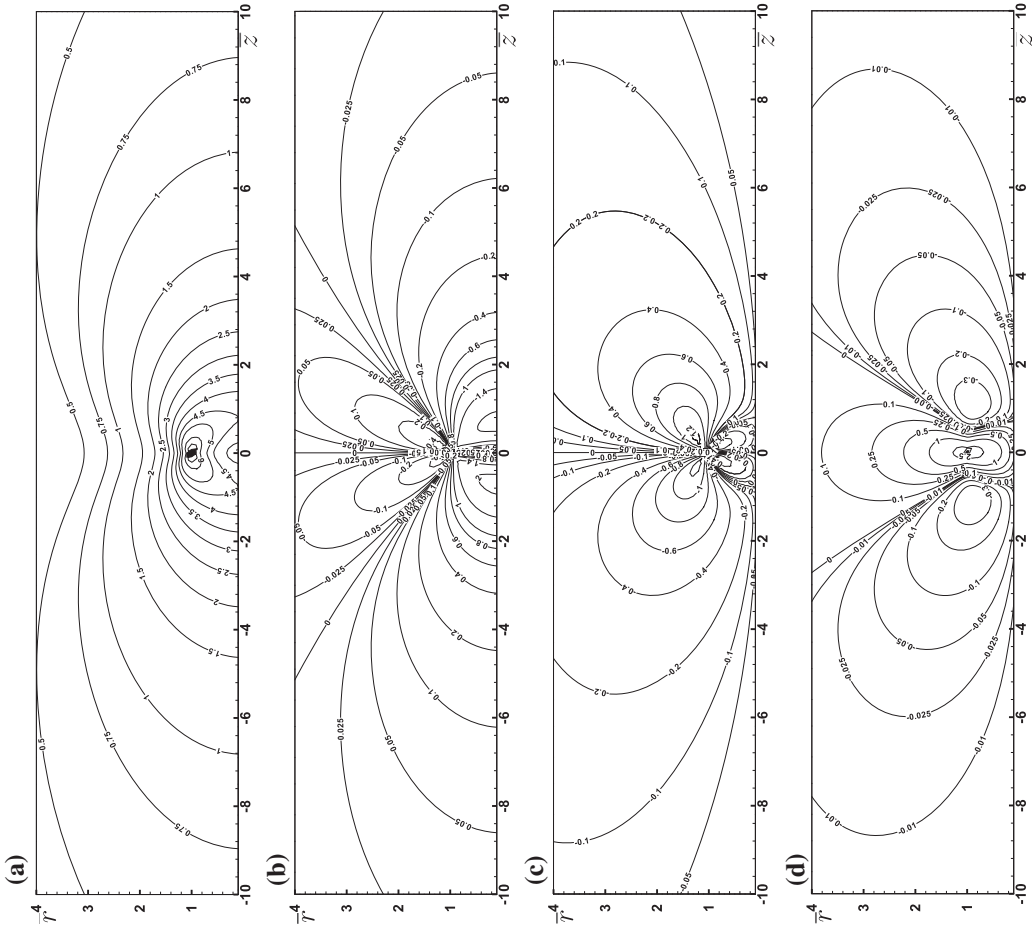


**Figure 2.** Isolevel contours of the normalised axial and radial velocity components of the axisymmetric fundamental flows for  $\bar{\tau}_0 = 1$ . (a):  $U_z^{(1)}$ . (b):  $U_z^{(2)}$ . (c):  $U_r^{(1)}$ . (d):  $U_r^{(2)}$ .

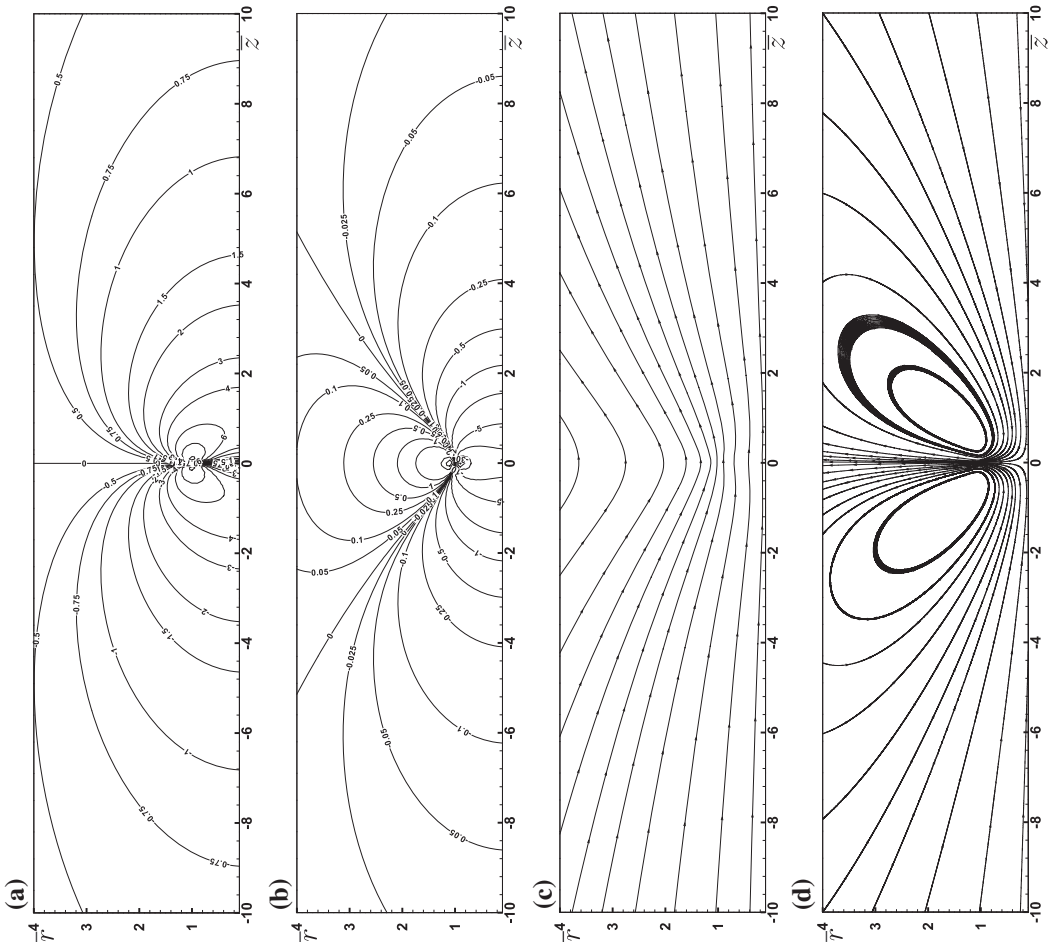


**Figure 3.** Normalised pressure isolevel contours and streamlines of the axisymmetric fundamental flows for  $\bar{r}_0 = 1$ . (a):  $p^{(1)}$ . (b):  $p^{(2)}$ . (c) First flow (axial forces) streamlines. (d) Second flow (radial forces) streamlines.

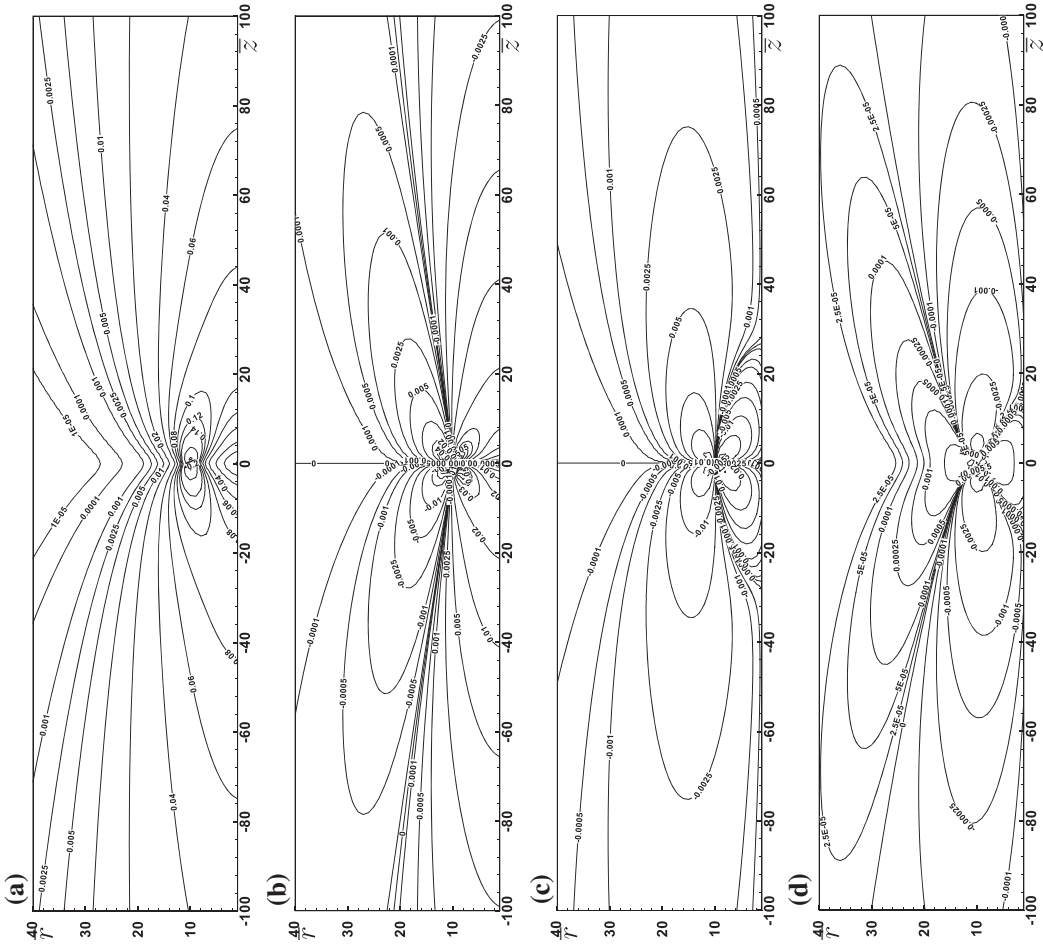


**Figure 4.** Isolevel contours of the normalised axial and radial velocity components of the axisymmetric fundamental flows for  $\bar{\tau}_0 = 10$ . (a):  $U_z^{(1)}$ . (b):  $U_z^{(2)}$ . (c):  $U_r^{(1)}$ . (d):  $U_r^{(2)}$ .

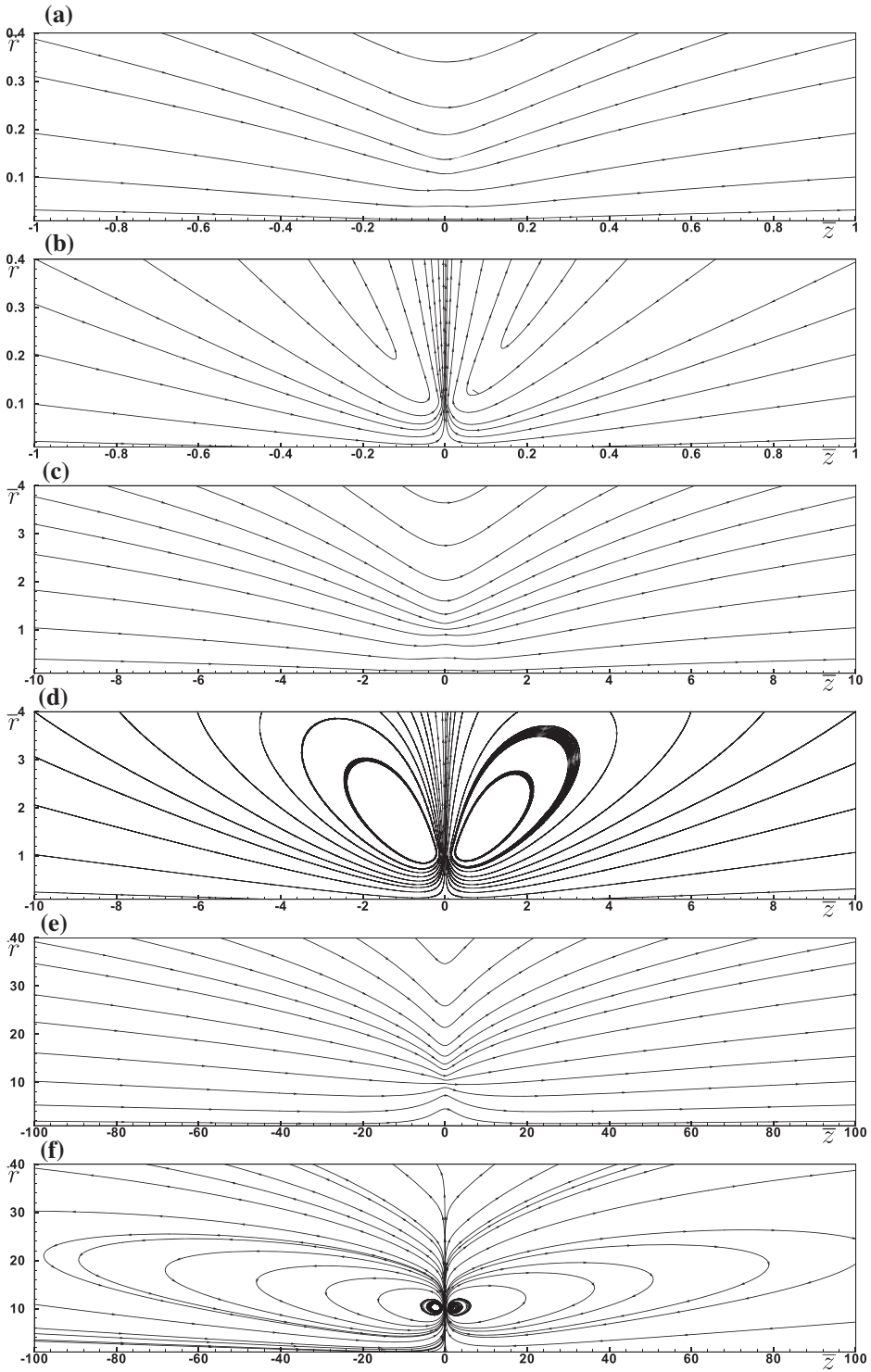


**Figure 5.** Fundamental axisymmetric flow streamlines for  $\bar{r}_0 = 0.1, 1, 10$ . The value of  $\bar{r}$  increases from top to bottom and the first fundamental flow (due to axial forces on the ring) is for cases (a), (c) and (e).

contours of the following normalised quantities (for  $l = 1, 2$ )

$$U_r^{(l)} = \left[ \frac{8\pi\mu d}{F} \right] u_r^{(l)}, \quad U_z^{(l)} = \left[ \frac{8\pi\mu d}{F} \right] u_z^{(l)}, \quad P^{(l)} = \left[ \frac{8\pi d^2}{F} \right] p^{(l)} \quad (65)$$

and the associated streamlines.

For a given value of  $\bar{r}_0$  the two fundamental flows exhibit quite different patterns. This is shown in Figure 2 for the normalised velocity components and  $\bar{r}_0 = 1$ .

This figure reveals that, not surprisingly, all these quantities are positive in the entire fluid half domain. Moreover,  $U_z^{(1)}$  is larger than  $U_z^{(2)}$ . These quantities and  $U_r^{(1)}$  decay slowly away from the ring trace point  $P$  having coordinates  $\bar{z} = 0$  and  $\bar{r} = 1$ . By contrast,  $U_r^{(2)}$  exhibit a very fast decay away from  $P$  and this explains why, amazingly, the velocity component  $U_r^{(2)}$  due to radial forces becomes smaller than the component  $U_r^{(1)}$  due do axial forces except in the very vicinity of the ring trace  $P$ . The same trend is observed for the normalised pressures in Figure 3.

Each resulting flow streamlines (which here coincide with the fluid particles trajectories since the flow is steady) are also drawn in Figure 3. It appears that for the second flow due to the ring radial force distribution some trajectories are closed near the ring trace point  $P$ . This means that some fluid particles located near the ring are trapped, i.e. not able to escape away as it is the case for the first fundamental flow produced by the ring axial forces.

We close this subsection by investigating the previous results sensitivity to the normalised ring radius  $\bar{r}_0$ . This is here done by considering, in Figure 4, the obtained velocity components for a large ring  $\bar{r}_0 = 10$ .

The trends (hierarchy and decay rate away from the ring trace) previously noticed for the ring with radius  $\bar{r}_0 = 1$  and depicted in Figure 2 still hold. Here the addressed fluid domain is larger, both in terms of  $\bar{z}$  and  $\bar{r}$ , than the one seen in Figure 2 and this permits one to observe non-necessary similar far-field behaviour of each normalised velocity component in directions close either to the  $\bar{z}$  axis or to the  $\bar{r}$  axis. It thus appears that near the two upstream and downstream directions ( $\bar{r} \sim 0$ ) the normalised velocity  $U_z^{(1)}$  experiences a very slow decay while the magnitude of other reported velocities (especially the quantity  $U_r^{(2)}$ ) quickly decrease in all directions away from the ring trace point  $P$ .

Finally, we gather in Figure 5 the computed fundamental flow streamlines for  $\bar{r}_0 = 0.1, 1, 10$ . On comparing the different plots, the reader should note that the pocket of trapped liquid for the second fundamental flow can extend far away from the ring (see the  $\bar{r}_0 = 10$  case).

## 5. Conclusions

The radial and axial velocity components ( $u_r, u_z$ ) and the pressure  $p$  of two basic fundamental *axisymmetric* MHD viscous flows produced in a conducting

Newtonian liquid by axial and radial distributions of forces on the  $(z - z_0)^2 + (r - r_0)^2 = 0$  ring in the presence of a given uniform axial magnetic field  $\mathbf{B} = B\mathbf{e}_z$ , with  $B > 0$ , have been obtained in closed form.

The adopted procedure requires to determine the pressure and some of the Cartesian components of a more involved *three-dimensional* fundamental MHD flow and permits one to get the required axisymmetric flows in closed form. At point  $(r, \theta, z)$  each flow solely depend upon both  $(r, r_0, z - z_0)$  and the so-called Hartmann layer thickness  $d = (\sqrt{\mu/\sigma})/B$ . The proposed numerical treatment, both implemented and tested, makes it possible to accurately compute the flow velocity components and pressure  $(u_r, u_z, p)$ . The resulting flow patterns, drawn versus the normalised coordinates  $\bar{r} = r/d$  and  $\bar{z} = z/d$ , reveal that both flows exhibit quite different behaviours at given parameters  $(r_0, d)$  and also deeply depend upon the ring-normalised radius  $\bar{r}_0 = r_0/d$ .

From the knowledge of  $(u_r, u_z, p)$  versus  $(r, z)$  it is straightforward to obtain, if needed, the resulting stress tensor components (again in cylindrical coordinates). This derivation offers no additional difficulty and is thus left to the reader.

As mentioned in the introduction, we intend in future to develop a new boundary element method to get the axisymmetric MHD flow about a translating axisymmetric body having axis of revolution and translational velocity parallel with the uniform magnetic field  $\mathbf{B}$ . Such a challenging task will appeal to the two axisymmetric fundamental flows (but not to the associated stress tensors!) obtained in the present paper. Since requiring additional efforts such investigations are however postponed to another work.

## Disclosure statement

No potential conflict of interest was reported by the authors.

## References

- Abramowitz, M. & Stegun, I. A. (1965). *Handbook of mathematical functions*. New York, NY: Dover Publications.
- Branover, G. G. & Tsinober, A. B. (1970). *Magnetohydrodynamic of incompressible media*. Moscow: Nauka.
- Chester, W. (1957). The effect of a magnetic field on Stokes flow in a conducting fluid. *Journal of Fluid Mechanics*, 3, 304–308.
- Chester, W. (1961). The effect of a magnetic field on the flow of a conducting fluid past a body of revolution. *Journal of Fluid Mechanics*, 10, 459–465.
- Dawson, T. W. (1995). On the singularity of the axially symmetric Helmholtz Green's function, with application to BEM. *Applied Mathematical Modelling*, 19, 590–601.
- Dini, F., Khorasani, S., & Amrollahi, R. (2004). Green function of axisymmetric magnetostatics. *Iranian Journal of Science & Technology, Transaction A*, 28(A2), 197–204.
- Gotoh, K. (1960). Magnetohydrodynamic flow past a sphere. *Journal of the Physical Society of Japan*, 15(1), 189–196.
- Gotoh, K. (1960). Stokes flow of an electrically conducting fluid in a uniform magnetic field. *Journal of the Physical Society of Japan*, 15(4), 696–705.

- Gradshteyn, I. S. & Ryzhik, Y. I. M. (1965). *Tables of Integrals, Series*. San Diego: And Products. Academic Press Inc.
- Happel, J. & Brenner, H. (1983). *Low Reynolds number hydrodynamics*. The Hague: Martinus Nijhoff Publishers.
- Hartmann, C. & Sanchez-Palencia, E. (1973). Limiting behaviour of a certain class of MHD flows in a strong magnetic field. *MagnetoHydrodynamics*, 1, 1–8.
- Hartmann, J. (1937). Theory of the laminar flow of an electrically conductive liquid in a homogeneous magnetic field. *Det Kgl. Danske Videnskabernes Selskab. Matematisk-fysiske Meddelelser*, XV(6), 1–28.
- Hasegawa, H. (1975). An extension of love's solution for the axisymmetric problems of elasticity. *Bulletin of the JSME*, 18(119), 484–492.
- Hasegawa, H. (1976). Axisymmetric body force problems of an elastic half-plane. *Bulletin of the JSME*, 19(137), 1262–1269.
- Hasegawa, H. (1981). On the stress concentration problem of a circular shaft with a semicircular groove under tension (an application of Green's function for body force problems of a solid cylinder). *Bulletin of the JSME*, 24(189), 520–527.
- Hasegawa, H. (1988). A fundamental solution and boundary element method for torsion problems of a bonded dissimilar elastic solid. Tanaka, M., & Cruse, T.A.. eds. *Boundary Element Methods in Applied Mechanics*. Chichester, UK: Wiley. (pp. 75–90)Chapter 5.
- Hasegawa, H. (1992). Green's functions for axisymmetric problems of dissimilar elastic solids. *Transactions of the ASME*, 59, 312–320.
- Hasegawa, H. (1984). Green's function for axisymmetric body force problems of an elastic half space and their application (an elastic half space with a hemispherical pit). *Bulletin of the JSME*, 27(231), 1829–1835.
- Kalis, K., Tsinober, A. B., Shtern, A., & Shcherbinin, E. V. (1965). Flow of a conducting fluid past a circular cylinder in a transverse magnetic fluid. *Magnitnaya Gidrodinamika*, 1(1), 18–28.
- Kermanidis, T. (1975). A numerical solution for axially symmetrical elasticity problems. *International Journal of Solids Structures*, 11, 493–500.
- Kim, S. & Karrila, S. J. (1983). *Microhydrodynamics*. The Hague: Principles and selected applications. Martinus Nijhoff Publishers.
- Moreau, R. (1990). *MagnetoHydrodynamics*. Fluid Mechanics and its Applications. Dordrecht: Kluwer Academic Publisher.
- Pozrikidis, C. (1992). *Boundary integral and singularity methods for linearized viscous flow*. Cambridge: Cambridge University Press.
- Priede, J. (2013). *Fundamental solutions of MHD Stokes flow*. arXiv:1309.3886v1. Physics. fluid. Dynamics.
- Priede, J. & Gerbeth, G. (2006). Boundary-integral method for poloidal axisymmetric AC magnetic fields. *IEEE Transactions On Magnetics*, 42(2), 1–8.
- Sellier, A. Boundary element technique for slow viscous flows about particles. *Boundary Element Methods in Engineering and Sciences*. Vol. 4. World Scientific, Chapter 7. pp. 239–281.
- Sellier, A., Aydin, S.H. & Tezer-Sezgin, M. (2014a). A new boundary approach for the 2D slow viscous MHD flow of a conducting liquid about a solid particle. *Advances in Boundary Element and Meshless Techniques XV*, (Florence, 2014), pp. 393–406
- Sellier, A., Aydin, S. H., & Tezer-Sezgin, M. (2014b). Free-space fundamental solution of a 2D steady slow viscous MHD flow. *CMES*, 102(5), 393–406.
- Tsinober, A. B. (1970). *MHD flow around bodies*. Fluid Mechanics and its Applications. Riga: Kluwer Academic Publisher.

Tsinober, A. B. (1973). Axisymmetric magnetohydrodynamic Stokes flow in a half-space. *Magnetohydrodynamics*, 4, 450–461.

Tsinober, A. B. (1973). Green's function for axisymmetric MHD Stokes flow in a half-space. *Magnetohydrodynamics*, 4, 559–562.

Yosinobu, H. (1960). A linearized theory of magnetohydrodynamic flow past a fixed body in a parallel magnetic field. *Journal of the Physical Society of Japan*, 15(1), 175–188.

Yosinobu, H. & Kabutani, T. (1959). Two-dimensional Stokes flow of an electrically conducting fluid in a uniform magnetic field. *Journal of the Physical Society of Japan*, 14(10), 1433–1444.

## Appendix 1. Functions $T_1$ and $T_2$

In this Appendix we give in closed form the functions  $T_1$  and  $T_2$  first occurring in (40)–(41). This is done using the distance  $R$  and the function  $g$  such that

$$R = |\mathbf{x} - \mathbf{x}_0|, \quad g(R, d) = e^{-R/(2d)}/R. \quad (\text{A1})$$

Appealing to (31) for  $\partial H/\partial x$ , we then have the following definitions

$$T_1 = g(R, d) \left\{ \frac{e^{(z-z_0)/(2d)}}{R - (z - z_0)} + \frac{e^{-(z-z_0)/(2d)}}{R + z - z_0} \right\} - \frac{2}{R^2 - (z - z_0)^2}, \quad (\text{A2})$$

$$T_2 = \frac{g(R, d)}{R} \left\{ \left[ \frac{R + 2d}{2dR} \right] \left[ \frac{e^{(z-z_0)/(2d)}}{R - (z - z_0)} + \frac{e^{-(z-z_0)/(2d)}}{R + z - z_0} \right] \right. \\ \left. + \frac{e^{(z-z_0)/(2d)}}{[R - (z - z_0)]^2} + \frac{e^{-(z-z_0)/(2d)}}{[R + z - z_0]^2} \right\} - \frac{4}{[R^2 - (z - z_0)^2]^2}. \quad (\text{A3})$$

Note that from (A1) we can recast the last terms appearing in  $T_1$  and  $T_2$  by using the relation

$$R^2 - (z - z_0)^2 = r^2 + r_0^2 - 2rr_0 \cos \theta_0 \quad (\text{A4})$$

so that both  $T_1$  and  $T_2$  solely depend upon  $(r, r_0, \theta_0, z - z_0)$  and  $d$ .

## Appendix 2. Expressing $I_{mn}$ in terms of elliptic integrals

Using the definitions (62) and the relation (63) easily yields the identities

$$I_{10} = \frac{2kF(k)}{(\bar{r} \bar{r}_0)^{1/2}}, \quad I_{20} = \frac{\pi k^2}{2\bar{r} \bar{r}_0 \sqrt{1 - k^2}}, \quad I_{30} = \frac{4k^3 E(k)}{(4\bar{r} \bar{r}_0)^{3/2} (1 - k^2)}, \quad (\text{B5})$$

$$I_{11} = \frac{2k}{(\bar{r} \bar{r}_0)^{1/2}} \left\{ \left( \frac{2}{k^2} - 1 \right) F(k) - \frac{2}{k^2} E(k) \right\}, \quad (\text{B6})$$

$$I_{21} = \frac{\pi}{2\bar{r} \bar{r}_0} \left\{ \frac{2 - k^2}{\sqrt{1 - k^2}} - 2 \right\}, \quad (\text{B7})$$

$$I_{31} = \frac{4k}{(4\bar{r} \bar{r}_0)^{3/2}} \left\{ \left[ \frac{2 - k^2}{1 - k^2} \right] E(k) - 2F(k) \right\}. \quad (\text{B8})$$

## Appendix 3. Alternative forms for $\bar{T}_1$ and $\bar{T}_2$

This Appendix provides the employed alternative forms used for the numerical implementation and of importance for  $\bar{r} = \bar{r}_0$ . By virtue of (A1)–(A3), the definitions of  $\bar{T}_1$  and  $\bar{T}_2$  immediately give

$$\bar{T}_1 = \frac{1}{\bar{R}} \left[ \frac{e^{-(\bar{R}-\bar{z})/2}}{\bar{R}-\bar{z}} + \frac{e^{-(\bar{R}+\bar{z})/2}}{\bar{R}+\bar{z}} \right] - \frac{2}{\bar{R}^2 - \bar{z}^2}, \quad (\text{C9})$$

$$\begin{aligned} \bar{T}_2 = \frac{1}{\bar{R}^2} \left\{ \left[ \frac{\bar{R}+2}{2\bar{R}} \right] \left[ \frac{e^{-(\bar{R}-\bar{z})/2}}{\bar{R}-\bar{z}} + \frac{e^{-(\bar{R}+\bar{z})/2}}{\bar{R}+\bar{z}} \right] \right. \\ \left. + \frac{e^{-(\bar{R}-\bar{z})/2}}{[\bar{R}-\bar{z}]^2} + \frac{e^{-(\bar{R}+\bar{z})/2}}{[\bar{R}+\bar{z}]^2} \right\} - \frac{4}{[\bar{R}^2 - \bar{z}^2]^2}. \end{aligned} \quad (\text{C10})$$

When  $\bar{R}^2 = \bar{z}^2$  the last terms on the right-hand sides of (C9)–(C10) induce numerical troubles. This basic issue is adequately handled using the following equivalent alternative forms:

$$\bar{T}_1 = \frac{1}{\bar{R}} \left[ \frac{e^{-(\bar{R}-\bar{z})/2} - 1}{\bar{R}-\bar{z}} + \frac{e^{-(\bar{R}+\bar{z})/2}}{\bar{R}+\bar{z}} \right] - \frac{1}{\bar{R}(\bar{R}+\bar{z})} \text{ for } \bar{z} > 0, \quad (\text{C11})$$

$$\bar{T}_1 = \frac{1}{\bar{R}} \left[ \frac{e^{-(\bar{R}+\bar{z})/2} - 1}{\bar{R}+\bar{z}} + \frac{e^{-(\bar{R}-\bar{z})/2}}{\bar{R}-\bar{z}} \right] - \frac{1}{\bar{R}(\bar{R}-\bar{z})} \text{ for } \bar{z} < 0, \quad (\text{C12})$$

$$\begin{aligned} \bar{T}_2 = \frac{1}{\bar{R}^2} \left\{ \left[ \frac{\bar{R}+2}{2\bar{R}} \right] \left[ \frac{e^{-(\bar{R}-\bar{z})/2}}{\bar{R}-\bar{z}} + \frac{e^{-(\bar{R}+\bar{z})/2}}{\bar{R}+\bar{z}} \right] \right. \\ \left. + \frac{e^{-(\bar{R}-\bar{z})/2} - 1}{[\bar{R}-\bar{z}]^2} + \frac{e^{-(\bar{R}+\bar{z})/2}}{[\bar{R}+\bar{z}]^2} \right\} - \frac{3\bar{R}+\bar{z}}{\bar{R}^2(\bar{R}+\bar{z})(\bar{R}^2 - \bar{z}^2)} \text{ for } \bar{z} > 0, \end{aligned} \quad (\text{C13})$$

$$\begin{aligned} \bar{T}_2 = \frac{1}{\bar{R}^2} \left\{ \left[ \frac{\bar{R}+2}{2\bar{R}} \right] \left[ \frac{e^{-(\bar{R}-\bar{z})/2}}{\bar{R}-\bar{z}} + \frac{e^{-(\bar{R}+\bar{z})/2}}{\bar{R}+\bar{z}} \right] \right. \\ \left. + \frac{e^{-(\bar{R}+\bar{z})/2} - 1}{[\bar{R}+\bar{z}]^2} + \frac{e^{-(\bar{R}-\bar{z})/2}}{[\bar{R}-\bar{z}]^2} \right\} - \frac{3\bar{R}-\bar{z}}{\bar{R}^2(\bar{R}-\bar{z})(\bar{R}^2 - \bar{z}^2)} \text{ for } \bar{z} < 0. \end{aligned} \quad (\text{C14})$$